

Distribution Method of Front/Rear Wheel Side-Slip Angles and Left/Right Motor Torques for Range Extension Control System of Electric Vehicle on Curving Road

Hayato Sumiya¹⁾ Hiroshi Fujimoto¹⁾

1) *The University of Tokyo, Graduate School of Frontier Sciences
Transdisciplinary Sciences Bldg., 5-1-5, Kashiwanoha,
Kashiwa, Chiba, 227-8561, Japan
(E-mail: sumiya@fujilab.k.u-tokyo.ac.jp, fujimoto@k.u-tokyo.ac.jp)*

Received on March 31st, 2011

Presented at the JSAE Annual Congress on May 17th, 2011

ABSTRACT: In this paper, the range extension control system based on least square method is proposed for electric vehicles with in-wheel motors and front active steering. This proposed method distributes front and rear wheel side-slip angles and driving force difference between left and right motors from lateral force and yaw-moment. The proposed method enables to reduce driving resistance generated from front steering angle. In fact, the mileage per charge is extended up to 200 m/kWh. Simulations and experiments are carried out to confirm the effectiveness of the proposed method.

KEY WORDS: Electric vehicle, Front active steering, Driving/braking force distribution

1. Introduction

Nowadays, the environmental problems as global warming, exhaustion of fossil fuels and air pollution are greatly paid attentions. For these problems, hybrid vehicles(HVs) and electric vehicles(EVs) are focused on. Especially, EVs are effective against prevention of global warming. In addition, EVs which are driven by electric motors has four advantages⁽¹⁾.

- Development of in-wheel motors enables individual control of each wheel.
- Continuous and smooth braking torque can be generated by regeneration.
- Generated torque can be measured precisely from motor current.
- Quick torque response is available by motor current control.

These advantages are effective for vehicle motion control. Author's research group has studied the slip-ratio control by using quick torque responses and vehicle motion control by using left and right driving force differences⁽²⁾⁽³⁾.

EVs which are superior to environmental problem has some issues to become widely used. Three issues are often taken up. First, EVs are more expensive than internal combustion engine vehicle(ICEV). Second, the number of charging facility are few. Finally, the mileage per charge is very short. Especially, the issue of mileage per charge depends on battery capacity. In order to solve this issue, the research on variable-parameter permanent-magnetic motors, which can change flux according to the speed and a novel drive method of motor, which is driven with high efficiency point by two reduction gear are studied⁽⁴⁾⁽⁵⁾. However, in order to solve this problem drastically, it is neces-

sary to improve battery capacity.

Author's research group proposed range extension control system(RECS) for solving the issue on mileage per charge⁽⁶⁾⁽⁷⁾⁽⁸⁾. In (6), it is assumed that EVs have two differential efficiency motors which are adopted front and rear wheels. When vehicle is running on straight road, torque distribution is realized by front and rear motors. It enables to reduce the total energy loss by distributing motors torque to optimal efficiency points of each motor. By the method, it is optimized from battery output to motor output. In (7) and (8), it is assumed that EVs enable individual control of left and right motors. When vehicle is running on curving road, front steering angle is reduced by using yaw-moment generated by torque difference between left and right motors. As a result, it is able to reduce driving resistance generated by front steering. Energy loss is reduced, because driving resistance is decreased. However, in (7) and (8), it is conducted minimization of mechanical output only, because electric loss is not considered.

In our group a distribution method was used equalization of work load for each wheel to stabilize vehicle motion⁽⁹⁾. However, in this paper, distribution method based on least square method is proposed for range extension control system. Proposed method enables to calculate front steering angle and yaw-moment generated by torque difference, which can minimize the driving resistance, from lateral force balanced in centrifugal force and yaw-moment. In addition, electric loss is added to cost function. As a result, it becomes possible to reduce both mechanical output and copper loss. The effectiveness of proposed method is verified by simulation and experiment.



(a) FPEV2-Kanon (b) In-wheel motor
Fig. 1 Experimental vehicle.

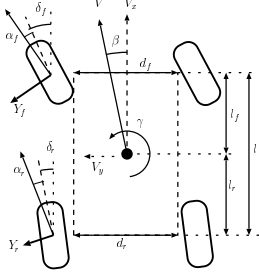


Fig. 2 Vehicle model.

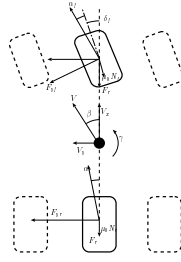


Fig. 3 Two vehicle model.

Table 1 Vehicle specification.

Dimensions(L×W×H)	2300×1600×1510 mm
Weight	850 kg
Vehicle yaw inertia	617 kgm ²
l_f	999 mm
l_r	701 mm
Tread base	1300 mm
Radius of tire	302 mm

2. Experimental vehicle

An original experimental EV “FPEV2-Kanon”, that is developed in the author’s laboratory, is used for performance verification. In this section, the characteristics of the experimental vehicle are explained. In-wheel motors, which are outer-rotor type, are installed in each wheel. Since this motor uses direct drive system, the reaction force from the road is directly transferred to the motor side without gear reduction and backlash. It is possible to generate yaw-moment by different driving force between left and right in-wheel motor. The steering mechanism adopts active front and rear steering system, by using two 250W DC motors for electric power steering (EPS). Moreover, in order to switch Steer-by-Wire (SbW) and EPS, the steering wheel shaft has a removable structure. In this paper, only two structures are used, one is the rear in-wheel motor, the other is front active steering.

Fig. 1(a) shows experimental vehicle, Fig. 1(b) shows in-wheel motor, Table 1 shows vehicle specifications.

3. Vehicle modeling

3.1. Vehicle dynamics

In this section, vehicle dynamics which describes four wheel drive and front and rear steering are explained⁽¹⁰⁾. Fig. 2 shows vehicle model. Wheel motion equation is represented by

$$J_\omega \frac{d\omega}{dt} = T - rF_d, \quad (1)$$

where J_ω is wheel inertia, ω is wheel speed, T is motor torque, r is tire radius, and F_d is driving force.

Longitudinal motion equation, lateral motion equation and yaw-dynamics equation are represented by

$$\begin{aligned} F_x &= F_{xfl} + F_{xfr} + F_{xrl} + F_{xrr}, \quad (2) \\ F_y &= MV(\dot{\beta} + \gamma) = F_{yfl} + F_{yfr} + F_{yrl} + F_{yrr}, \quad (3) \\ M_z &= I\dot{\gamma} = F_{yfl}l_f + F_{yfr}l_f - F_{yrl}l_r - F_{yrr}l_r \\ &\quad + \frac{d_f}{2}(-F_{xfl} + F_{xfr}) + \frac{d_r}{2}(-F_{xrl} + F_{xrr}). \quad (4) \end{aligned}$$

where F_x is vehicle driving force, F_y is lateral force, M_z is yaw-moment acting on vehicle center of gravity, F_{xfl} , F_{xfr} , F_{xrl} and F_{xrr} are driving forces generated each wheel, F_{yfl} , F_{yfr} , F_{yrl} and F_{yrr} are lateral forces generated each wheel, M is vehicle mass, β is vehicle side-slip angle, γ is yaw-rate, I is vehicle yaw inertia, l_f and l_r are the distance from body center of gravity to steering knuckle spindle, and rear wheel axle, respectively, and d_f and d_r are tread bases of front and rear axle, respectively.

Wheel side-slip angles are angles between wheel traveling direction and wheel rotation direction. These are represented by α_{fl} , α_{fr} , α_{rl} and α_{rr} , respectively. Cornering forces Y_f and Y_r are perpendicular force against this wheel traveling direction. If left and right tire characteristics are the same and front and rear steering angles are small, lateral forces generated by left and right tire are same. In addition, it is assumed that lateral force equal with cornering force. In this condition, the relationships of wheel side-slip angles, lateral forces, and cornering forces are represented by

$$\alpha_{fl} \simeq \alpha_{fr} \simeq \alpha_f = \beta + \frac{l_f\gamma}{V} - \delta_f, \quad (5)$$

$$\alpha_{rl} \simeq \alpha_{rr} \simeq \alpha_r = \beta - \frac{l_r\gamma}{V} - \delta_r, \quad (6)$$

$$F_{yfl} \simeq F_{yfr} \simeq F_{yf} \simeq Y_f = -C_f\alpha_f, \quad (7)$$

$$F_{yrl} \simeq F_{yrr} \simeq F_{yr} \simeq Y_r = -C_r\alpha_r, \quad (8)$$

where V is vehicle velocity, and C_f and C_r are cornering stiffness.

3.2. Driving resistance

In this section, driving resistance is explained. This occurs by front steering when vehicle is running on curving road. Fig. 3 shows bicycle model. This model is assumed that left and right tire characteristics are the same. Tires generate lateral forces and rolling friction when vehicle is running. Longitudinal elements of these forces and disturbances such as wind and road condition become driving resistance F_r . Driving resistance F_r is represented by

$$F_r = 2F_{yf} \sin \delta_f + \mu_0 N_f \cos \alpha_f + \mu_0 N_r \cos \alpha_r + F_{dis}, \quad (9)$$

where F_{dis} is disturbances such as wind and road condition, μ_0 is coefficient of rolling friction, N_f and N_r are front and rear vertical forces.

4. Distribution method based on least square method

4.1. Cost function

In this section, the cost function is defined to minimize the total loss. In this paper, it is assumed that rear-wheel-drive vehicle has front active steering unit. Therefore, front driving force and rear steering angle are treated 0. Power loss which becomes cost function is derived. Power loss P , which generated by EV driven by electric motor, compose 3 elements. 3 elements are mechanical output P_m , copper loss P_c , and iron loss P_i .

$$P = P_m + P_c + P_i \quad (10)$$

Here iron loss P_i is ignored for simplification. Mechanical output is generated by product of torque and wheel speed. It is assumed that torque is controlled by $i_d = 0$ control, copper loss is generated in proportion to the square of q axis current i_q of permanent magnetic motor.

$$P_m = T_{rl}\omega_{rl} + T_{rr}\omega_{rr} \quad (11)$$

$$P_c = R_{arl}i_{qrl}^2 + R_{arr}i_{qrr}^2 \quad (12)$$

where i_{qrl} and i_{qrr} are q axis current carrying left and right motor, and R_{arl} and R_{arr} are armature winding resistance of left and right motor.

First, mechanical output is derived. It is assumed that all wheels adhere to road. In this condition, mechanical output is represented by

$$P_m = F_x V_x + N_z \gamma, \quad (13)$$

where V_x is longitudinal velocity, N_z is yaw-moment generated by torque difference between left and right motors.

Second, copper loss is derived. Copper loss is generated in proportion to the square of q axis current i_q . Q -axis current i_q is able to derive from torques.

$$i_q = \frac{T}{P_n \phi_a} = \frac{T}{K_t} \quad (14)$$

where P_n is number of pairs of poles, ϕ_a is interlinkage magnetic flux, and K_t is torque constant. Next, torques of each wheel are derived. Considering that wheel speed ω is constant on steady state, the relationship between torque and driving force is represented by

$$T = rF_d. \quad (15)$$

Driving force and yaw-moment generated by torque difference between left and right motors are distributed equally to left and right motors.

$$\begin{bmatrix} F_{rl} \\ F_{rr} \end{bmatrix} = \begin{bmatrix} \frac{1}{2} & -\frac{1}{d_r} \\ \frac{1}{2} & \frac{1}{d_r} \end{bmatrix} \begin{bmatrix} F_x \\ N_z \end{bmatrix} \quad (16)$$

Left and right armature winding resistances and torque constants are the same because same motors are installed.

$$R_{arl} = R_{arr} = R_a \quad (17)$$

$$K_{trl} = K_{trr} = K_t \quad (18)$$

Therefore, copper loss is derived by substituting (14)~(18) for (12), and represented by

$$P_c = \frac{R_a r^2}{K_t^2} \left(\frac{1}{2} F_x^2 + \frac{2}{d_r^2} N_z^2 \right). \quad (19)$$

The sum of (13) and (19) is power loss.

Public road is usually composed of straight road and curving road. Moreover, curving road is constructed of some circles with different radius. Therefore, in this paper, it is assumed that vehicle is running steady circle turning with constant velocity and constant yaw-rate. Driving force needs the same value of the driving resistance to turn with constant velocity. Mechanical output and copper loss are substituted (9) for (13) and (19) when vehicle is running on curving road.

$$P_m = (2F_{yf} \sin \delta_f + \mu_0 N_z \cos \delta_f + \mu_0 N_r) V_x + N_z \gamma \quad (20)$$

$$P_c = \left(\frac{R_a r^2}{2K_t^2} (2F_{yf} \sin \delta_f + \mu_0 N_z \cos \delta_f + \mu_0 N_r)^2 + \frac{2R_a r^2}{K_t^2 d_r^2} N_z^2 \right) \quad (21)$$

4.2. Distribution method based on least square method

Lateral motion equation (3) and yaw-dynamics equation (4) are organized as

$$\begin{bmatrix} -2C_f & -2C_r & 0 \\ -2C_f l_f & 2C_r l_r & 1 \end{bmatrix} \begin{bmatrix} \alpha_f \\ \alpha_r \\ N_z \end{bmatrix} = \begin{bmatrix} F_y \\ M_z \end{bmatrix}, \quad (22)$$

where left-hand side coefficient matrix is defined as \mathbf{A} , vector of wheel side-slip angles and yaw-moment generated by torque difference between left and right motors is defined as $\mathbf{x} = [\alpha_f \ \alpha_r \ N_z]^T$, right-hand side vector $[F_y \ M_z]^T$ is defined as \mathbf{b} . Cost function J is derived that rolling friction is neglected and front steering angle is approximated enough small.

$$J = 2F_{yf} \delta_f V_x + N_z \gamma + \frac{2R_a r^2}{K_t^2} F_{yf}^2 \delta_f^2 + \frac{2R_a r^2}{K_t^2 d_r^2} N_z^2 \quad (23)$$

Cost function J is minimized by distribution of front and rear wheel side-slip angle and yaw-moment generated by torque difference. Therefore, it is necessary that front steering angle δ_f is represented by front and rear wheel side-slip angle α_f and α_r . Front steering angle δ_f is represented by substituting (5) for (6).

$$\delta_f = \frac{l}{V} \gamma - (\alpha_f - \alpha_r) \quad (24)$$

In addition, yaw-rate γ of lateral motion equation (3) is substituted for (24). In this paper, time derivative of vehicle side-slip angle β is assumed to be zero, because steady circle turning is assumed. Then, from (3), yaw-rate γ is represented by

$$\gamma = \frac{-2C_f \alpha_f - 2C_r \alpha_r}{MV}. \quad (25)$$

Therefore, (7), (24), and (25) is substituted for (23).

$$J \simeq \left(\frac{4C_f^2 l}{MV} + 2C_f V \right) \alpha_f^2 + \left(\frac{4C_f C_r l}{MV} - 2C_f V \right) \alpha_f \alpha_r - \frac{2C_f}{MV} \alpha_f N_z - \frac{2C_r}{MV} \alpha_r N_z + \frac{2R_a r^2}{K_t^2 d_r^2} N_z^2 \quad (26)$$

In this paper, α_f^4 , $\alpha_f^2 \alpha_r^2$, $\alpha_f^2 N_z$, and $\alpha_f \alpha_r N_z$ are enough

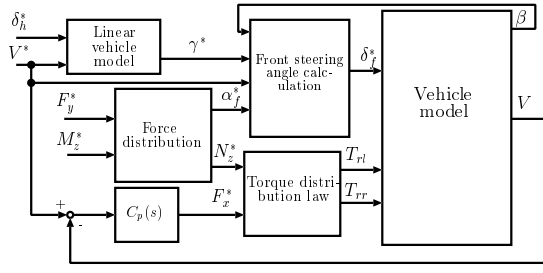


Fig. 4 Block diagram of range extension control system with least square solution.

small, and these values are ignored, because minimization is conducted by least square method. Higher order terms more than 3rd order of J are generated to substitute driving force which balanced with driving resistance for (23). (26) is equal to only copper loss which generated by mechanical output and yaw-moment generated by torque difference between left and right motor, because these values are approximated as enough small.

In addition, \mathbf{W} is defined as weighting matrix. Weighted least square solution \mathbf{x}_{opt} is represented by

$$J = \mathbf{x}^T \mathbf{W} \mathbf{x}, \quad (27)$$

$$\mathbf{x}_{opt} = \mathbf{W}^{-1} \mathbf{A}^T (\mathbf{A} \mathbf{W}^{-1} \mathbf{A}^T)^{-1} \mathbf{b}, \quad (28)$$

$$\mathbf{W} = \begin{bmatrix} \frac{4C_f^2}{MV}l + 2C_fV & \frac{2C_fC_r}{MV}l - C_fV & -\frac{C_f}{MV} \\ \frac{2C_fC_r}{MV}l - C_fV & 0 & -\frac{C_r}{MV} \\ -\frac{C_f}{MV} & -\frac{C_r}{MV} & \frac{2R_a r^2}{K_t^2 d_r^2} \end{bmatrix}. \quad (29)$$

Lateral force and yaw-moment are used as references, front and rear wheel side-slip angles and yaw-moment generated by torque difference between left and right motors which minimized J is calculated by (28). References of front steering angle and left and right torques are generated by these values.

5. Simulation

Fig. 4 shows block diagram of range extension control system used in simulation. In conventional method, vehicle turns used only front steering angle. In proposed method, vehicle turns used front and rear wheel side-slip angles and yaw-moment generated by torque difference between left and right motors which calculated by (28). Both conventional method and proposed method are conducted steady circle turning. These are compared by sum of mechanical output based on (11) and copper loss based on (12). Vehicle velocity controller is designed to keep the constant velocity. Proportional gain in the vehicle velocity controller is designed by pole placement method. The plant of vehicle velocity controller is considered as vehicle mass.

$$V = \frac{1}{Ms} F_x \quad (30)$$

The pole of vehicle velocity controller is -5 rad/s. Vehicle velocity controller $C_p(s)$ corresponds driver model. Driv-

ing force controlled by $C_p(s)$ and yaw-moment generated by torque difference between left and right motors calculated by (28) is used as left and right torque inputs by (16). In this paper, front wheel side-slip angle α_f^* control is used only, because experimental vehicle which enables front active steering is assumed. Reference of front steering angle δ_f^* is calculated from α_f^* by below equation.

$$\delta_f^* = \beta + \frac{l_f \gamma^*}{V^*} - \alpha_f^* \quad (31)$$

Vehicle velocity V^* of (31) is used vehicle velocity input. Yaw-rate γ^* is calculated by vehicle linear model from front steering angle δ_h^* and vehicle velocity V^* (10). δ_h^* is a front steering angle which is needed to turn by conventional method. Moreover, vehicle side-slip angle β is used a vehicle output. Reference of lateral force F_y^* which used in proposed method is calculated from circle radius, vehicle velocity, and vehicle mass. It is represented by

$$F_y^* = \frac{MV^2}{R}, \quad (32)$$

where R is circle radius. The circle radius in which vehicle is running with conventional method is used. In addition, reference of yaw-moment is $M_z^* = 0$. This is because yaw-rate is constant.

The simulation model is used “2D-TireModel ver1.0” (11). The nominal values of front and rear cornering stiffness are $C_f = 8000$ N/rad and $C_r = 15000$ N/rad, respectively. Simulation conditions are $V = 15$ km/h and $R = 8$ m. Both conventional method and proposed method are measured during 15 s. Moreover, each result is compared by average values. Fig. 5 shows simulation results. Front steering angle is reduced by proposed method as shown in Fig. 5(a). This is because lateral force, which is necessary when the vehicle is turning, is distributed by the proposed method. The yaw-moment generated by torque difference between left and right motors is shown in Fig. 5(b). The yaw-moment which becomes insufficient with proposed method is compensated by yaw-moment generated by torque difference between left and right motors. Fig. 5(c) and Fig. 5(d) show vehicle velocity and vehicle trajectory, respectively. From these results, it is able to confirm that both conventional method and proposed method are turning with constant velocity and at the same circle radius. Fig. 5(e) shows average values of power loss and Fig. 5(f) shows magnified figure of it. This power loss is sum of both mechanical output and copper loss. Power loss is reduced 5% with proposed method.

Table 2 shows km per kWh. In this paper, the efficiency of chopper, inverter and motor are treated as 100 %. Running distance in 15 s is integrated the vehicle velocity with simulation time. In a similar way, energy is integrated power loss with simulation time. Moreover, km per kWh is calculated to divide run distance by energy. Capacity of

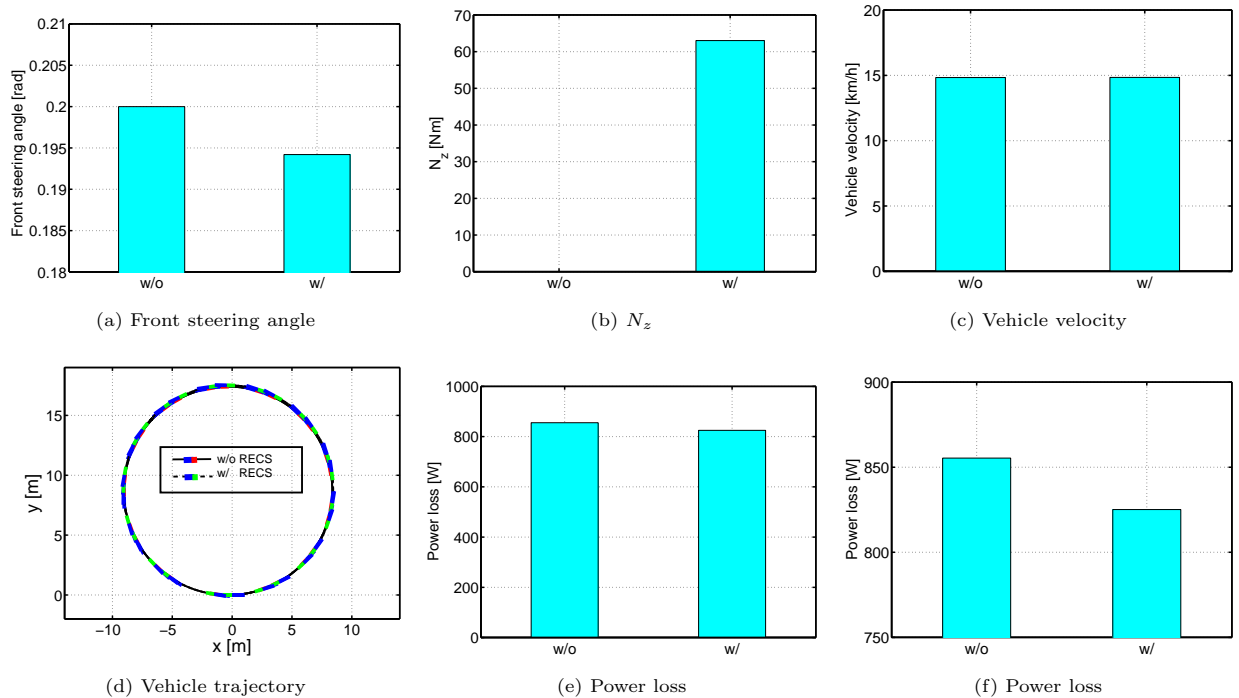


Fig. 5 Simulation results.

Table 2 km per kWh (simulation results).

Battery capacity	Without RECS	With RECS
1 kWh	17.4 km	18.0 km
5 kWh	87.0 km	90.0 km
16 kWh	278.4 km	288.0 km

Table 3 km per kWh (experimental results).

Battery capacity	Without RECS	With RECS
1 kWh	8.03 km	8.20 km
5 kWh	40.19 km	41.01 km
16 kWh	128.61 km	131.23 km

batteries are assumed 5 kWh for experimental vehicle and 16 kWh for the i-MiEV produced by MISTUBISHI MOTORS⁽¹²⁾. The run distance is extended to 600 m per 1 kWh with proposed method.

6. Experiment

Experiment is carried out under same condition with simulation. Experimental vehicle, shown in section 2, is used. Experiment is conducted in parking area of university. Experimental conditions are vehicle velocity $V = 15$ km/h and circle radius $R = 8$ m. Both conventional method and proposed method are examined at steady circle turning. In experiment, power loss is product value of inverter input voltage V_{dc} and inverter input current I_{dc} . This result includes not only mechanical output and copper loss but iron loss and efficiency of inverter and motor. In order to confirm repeatability of experimental results, average values of 10 times of both conventional method and proposed method are used. Moreover, standard deviation $\pm\sigma$ of each result is shown as error bar.

Fig. 6 shows experimental results. Front steering angle is reduced and yaw-moment, generated by torque difference between left and right motors, is generated by proposed method as shown in Fig. 6(a) and Fig. 6(b). It is confirmed that yaw-moment which becomes insufficient with proposed method is compensated by yaw-moment generated by torque difference between left and right motors. Both conventional method and proposed method have the same velocity as shown in Fig. 6(c). Fig. 6(d) shows vehicle trajectory. The vehicle trajectory of proposed method is larger than that of conventional method. This is because yaw-rate is reduced slightly by distribution. However, power loss which reduces of yaw-rate corresponds about 0.1 W. The power loss is reduced almost 50 W by the proposed method as shown in Fig. 6(e) and Fig. 6(f). Therefore, there is enough effectiveness even if this power loss is considered. Power losses are calculated from measured inverter inputs. It is confirmed that power loss is reduced about 3% by proposed method.

Table 3 shows km per kWh calculated in similar way of simulation. Mileage per charge is extended 200 m per 1kWh as shown in Table 3. However, efficiency of experimental results is less than one of simulation results. This is because experimental results include iron loss, motor efficiency and inverter efficiency.

7. Conclusion

In this paper, distribution method of lateral force and yaw-moment for range extension control system is proposed. It is confirmed that proposed method enables to extend mileage per charge by simulation and experiment.

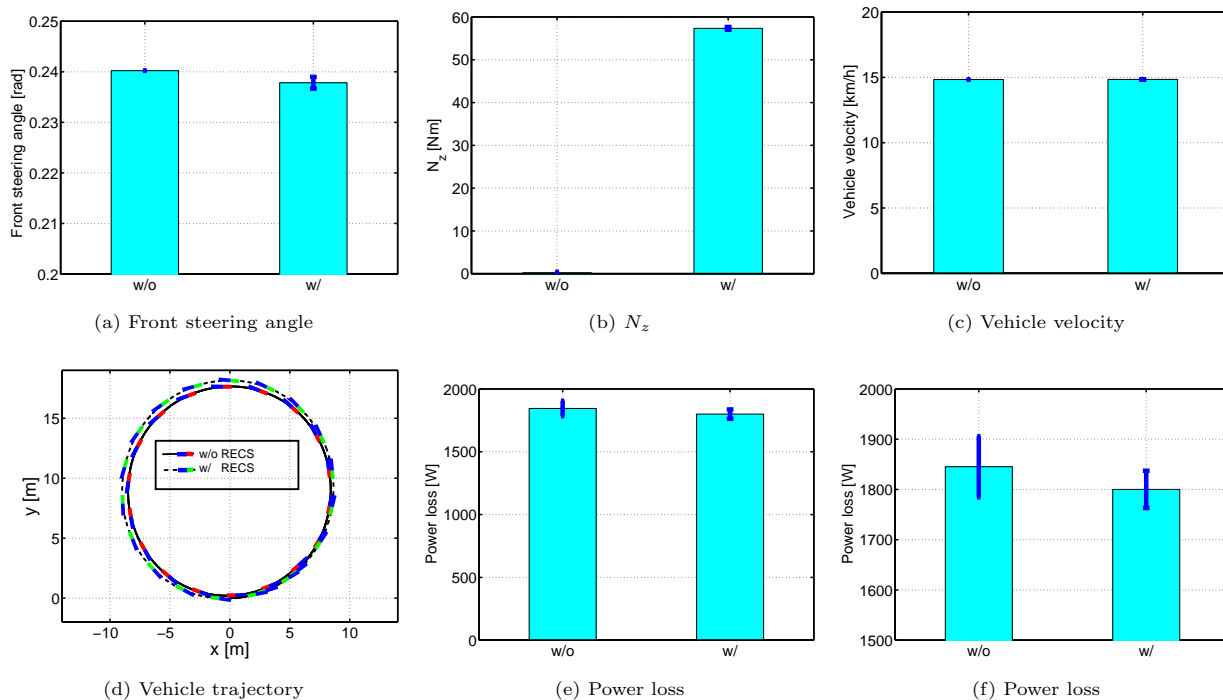


Fig. 6 Experimental results.

The future works will be evaluation using other turning methods.

Acknowledgment

Finally, this research was partly supported by Industrial Technology Research Grant Program from New Energy and Industrial Technology Development Organization (NEDO) of Japan and in part by the Ministry of Education, Culture, Sports, Science and Technology grant number 22246057.

References

- (1) Yoichi Hori: "Future Vehicle by Electricity and Control-Reserch on Four-Wheel-Motored: UOT Electric March II", IEEE Trans. IE, Vol.51. No.5. 2004
- (2) Toru Suzuki, Hiroshi Fujimoto: "Slip Ratio Estimation and Regenerative Brake Control for Decelerating Electric Vehicles without Detection of Vehicle Velocity and Acceleration", Trans. IEE of Japan, Vol. 130, no. 4, pp.512-517, 2010
- (3) Yuya Yamauchi, Hiroshi Fujimoto: "Vehicle Motion Control Method Using Yaw-moment Observer and Lateral Force Observer for Electric Vehicle", Trans. IEE of Japan, vol.130, no. 8, pp.939-944, 2010
- (4) Kazuto Sakai, Kazuaki Yuki, Yutaka Hashiba, Norio Takahashi: "Principle and Basic Characteristics of the Variable-Magnetic-Force Memory Motor", JIASC09, pp.179-184, 2009 (in Japanese)
- (5) Aldo Sornioti, Marco Boscolo, Andy Turner, Carlo Cavallino: "Optimisation of a 2-Speed Gear box for an Electric Vehicle", Proc. 10th International Symposium on Advanced Vehicle Control, pp.755-760, 2010
- (6) Toru Suzuki, Hiroshi Fujimoto, "Proposal of Range Extension Control System by Drive and Regeneration Distribution Based on Efficiency Characteristic of Motors for Electric Vehicle", IEE of Japan Technical Meeting Record, pp. 23-28, 2010 (in Japanese)
- (7) Hayato Sumiya, Hiroshi Fujimoto: "Range Extension Control System for Electric Vehicle with Active Front Steering and Driving/Braking Force Distribution on Curving Road", in Proc. 36th Annual Conference of the IEEE Industrial Electronics Society, pp.2346-2351, 2010
- (8) Hayato Sumiya, Hiroshi Fujimoto: "Range Extension Control System for Electric Vehicle with Active Front/Rear Steering and Driving/Braking Force Distribution on Curving Road", IEE of Japan Industry Applications Society Conference, Vol.2, pp.II-229-302, 2010 (in Japanese)
- (9) Naoki Ando, Hiroshi Fujimoto: "Distribution and Control Methods of Driving/Braking Force and Lateral Force for Electric Vehicle with Lateral-force Sensors and In-wheel Motors in All-wheels and Active Front/Rear Steering", IEE of Japan Technical Meeting Record, pp. 29-34, 2010 (in Japanese)
- (10) R. Rajamani: "Vehicle Dynamics and Control", Springer Science & Business Media, Inc., 2006
- (11) Shin-ichiro Sakai: "2D-TireModel ver 1.0", [http : //sakai.nnl.isas.ac.jp/index-j.html](http://sakai.nnl.isas.ac.jp/index-j.html), 2000
- (12) Makoto Kamachi, Hiroaki Miyamoto, Hiroaki Yoshida: "Development of Electric Vehicle for On-road Test", Proc. 8th International Symposium on Advanced Vehicle Control, pp.665-669, 2008